



Development of a low stress RF MEMS double-cantilever shunt capacitive switch

Hamid Reza Ansari¹ · Zoheir Kordrostami¹

Received: 23 February 2020 / Accepted: 30 March 2020 / Published online: 16 April 2020
© Springer-Verlag GmbH Germany, part of Springer Nature 2020

Abstract

In this paper, a novel RF MEMS shunt capacitive switch with application in the Ka frequency band is proposed. The spring design and the step structure added to the beam succeeded in improving the performance of the switch and reducing the stress which results in extended life-time of the switch. Also, by optimally reducing the gap between the dielectric and the beam (without problems such as self-actuation), the actuation voltage of the switch is significantly reduced. Electromechanical and scattering parameters analysis have been done by using COMSOL Multiphysics and HFSS software, respectively. The actuation voltage of the proposed device is 9.2 V. Since the aluminum has a lower mass compared to gold, an aluminum beam has been used in the switch. Desirable scattering parameters at the resonance frequency of 33.5 GHz have been obtained which include insertion loss of -0.3 dB and return loss of -18 dB. The high isolation of -57 dB verifies the improved performance of the switch. Finally, as another innovation in this paper, the effect of inductor and capacitor presence in the input of transmission line is investigated. This analysis has been done by using ADS. Results of the circuit analysis presented in this paper, help the MEMS switch designers to understand the realistic switch behavior before fabrication which considerably saves cost and time.

1 Introduction

In recent years, the use of RF MEMS switches as an alternative to p-i-n diodes and FET switches has become increasingly important due to the application of MEMS technology in the military and aerospace industries, urban order control, industrial factories and electronic devices (Rebeiz 2003; Amiri and Kordrostami 2018). Advantages such as low power consumption, small size, and high isolation have attracted attentions of scientists to research on MEMS-based technologies (Sravani et al. 2019a, b; Mafinejad et al. 2015). These switches can also be used in different frequency bands depending on their structures (Ansari and Behnam Taghaddosi 2019; Kordrostami and Roohizadegan 2018). Another case that distinguishes MEMS switches from other similar devices is their excellent performance at high frequencies compared to poor performance of solid-state based switches (Rebeiz et al. 2009; Kordrostami and Roohizadegan 2019). For the

design of an optimal MEMS device, researchers face challenges such as low actuation voltage, low stress, high isolation, good quality factor, low damping ratio, high switching speed, low power consumption, low weight and small size (Rao et al. 2019; Ansari and Khosroabadi 2018; Uvarov and Kupriyanov 2018).

In the literature, reduction of actuation voltage has been done by some methods such as the use of materials with high electrical conductivity and low mass, reduction of spring stiffness constant, and increasing the cross-sectional area of beam and dielectric layer, but most of them result in some disadvantages in switch characteristics (Ansari and Khosroabadi 2019; Mafinejad et al. 2017; Anuroop et al. 2018). The practical considerations have to be taken into account in designing a MEMS switch to avoid problems such as self-actuation and unstable springs (vibration of the springs) (Kordrostami and Roohizadegan 2019). Perforating the bridges reduces the mass of the beam which leads to an increase in the switching speed and in turn pulls the air under the membrane during pull-in operation (Ghoddus et al. 2019; Shekhar et al. 2017; Rebeiz 2003). The proposed structure in this paper, can overcome the large geometry, high power consumption and isolation challenges mentioned above (Rao et al. 2019; Molaei and Ganji 2017;

✉ Zoheir Kordrostami
kordrostami@sutech.ac.ir

¹ Department of Electrical and Electronics Engineering, Shiraz University of Technology, Shiraz, Iran

Khodadady and Azizolla 2015). The proposed spring design provides low cross-sectional area and good scattering parameters. Many previous works in the field of MEMS switches have used spring with low stiffness constant and low thickness to reduce the actuation voltage, which causes problems such as loosening of the spring or adhering of the beam to the dielectric layer which prevents from pull-up operation (Lakshmi et al. 2016; Mafinejad et al. 2019). But in the proposed switch by using a special spring design with a stiffness constant of 14.4 which is high (compared to previous work), a desired actuation voltage has been obtained. The high spring stiffness constant results in a high quality factor. In addition, in some previous works, the gap between the beam and the dielectric layer has been reduced to less than $0.7 \mu\text{m}$ to reduce the actuation voltage. But this will cause the beam to be automatically actuated and goes to the ON-state with shaking the device (Rebeiz 2003; Ghoddus and Kordrostami 2018). The proposed structure uses a step structure that changes from $0.7 \mu\text{m}$ to $2.8 \mu\text{m}$ in order to solve this problem. Switching time analysis is discussed to find out when the device switches from up-state to down-state. The proposed spring structure in this paper is very close to the spring structure in reality. The spring has two connected parts in two parallel planes with height differences. In this type of design, when the force is applied, the spring is stretched in the vertical direction and distributes the pressure along the helical parts of the spring which minimizes the stress on the spring. The proposed device also increases the lifetime of the switch even without the use of processes such as packaging. Practical MEMS switches are placed in an electrical circuit in the presence of a large number of passive and active elements, and consequently, these elements affect the performance of the switch. This effects have not been studied in previous works. However in this paper, in order to understand the behavior of the switch in a realistic situation, we analyzed the switch performance in the presence of two circuit elements (inductor and capacitor). The effects of inductors and capacitors with different inductances and capacitances on the switch isolation has been investigated. This study lets the researchers understand the switch characteristics in an electrical circuit before starting MEMS fabrication process and thus saves considerable cost and time.

The rest of the paper has been organized as follows. In Sect. 2, the structure design and dimensions of the proposed switch have been explained. In Sect. 3, the special spring structure has been explained. The characteristics of the switch such as the actuation voltage, capacitive ratio, resonance frequency, switching and release time, damping ratio, quality factor, high frequency performance analysis and the effect of inductor and capacitor on the switch isolation have been discussed in this section in detail. Finally, the paper has been concluded in Sect. 4.

2 Switch design

Generally, the performance of each RF MEMS switch has to be evaluated in both up and down state. The schematic diagram of the proposed RF MEMS switch when no pull-in voltage is applied to the beam (UP-state) is shown in Fig. 1.

After the voltage is applied, the beam is actuated by an electrical field and come into contact with a dielectric layer (DOWN-state) as shown in Fig. 2. The proposed RF MEMS switch has been placed upon a coplanar waveguide (CPW) line with a dimension of $80 \times 80 \times 80 \mu\text{m}$ and both sides of the switch have been fixed on the ground. The switch beam has been suspended using two anchors on top of the CPW. A dielectric layer is used to prevent metal-to-metal (M-to-M) contact between the beam and the transmission line (T-line). The proposed switch is a double-cantilever type switch that is connected to the springs with a height difference of $0.8 \mu\text{m}$ from the dielectric layer. Aluminum nitrate (AlN) and silicon have been used as dielectric layer and substrate, respectively. The reason for using AlN is because of its high dielectric constant, which results in increased capacitance ratio and improved high frequency performance. Aluminum has been chosen as the membrane because it has high electrical conductivity and low mass which result in good scattering parameters and low actuation voltage, respectively. The dimensions and

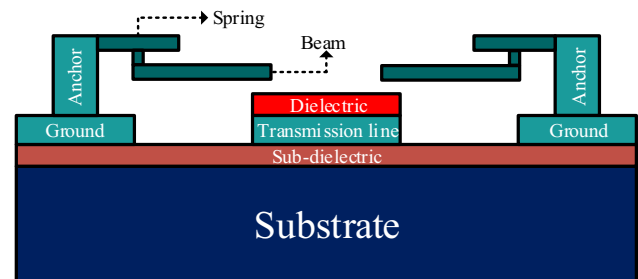


Fig. 1 The schematic of the proposed device before applying the pull-in voltage (UP-state)

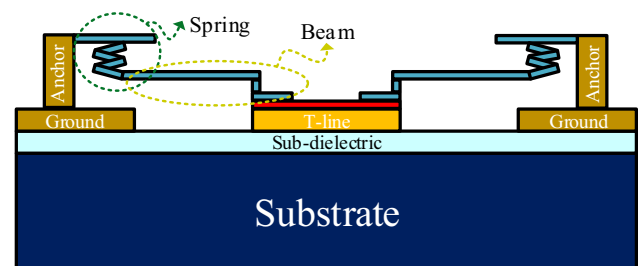


Fig. 2 The schematic of the proposed device after applying the pull-in voltage (DOWN-state)

Table 1 The characteristics of the MEMS device

Parameter	Width (μm)	Depth (μm)	Height (μm)	Material
Substrate	320	200	300	Silicon
Dielectric layer	80	68	0.1	AlN
CPW	80	200	2	Al
Bridge	2*15	65	0.8	Al
Oxide layer	320	200	2	SiO ₂
Hole dimension	10	10	0.8	–

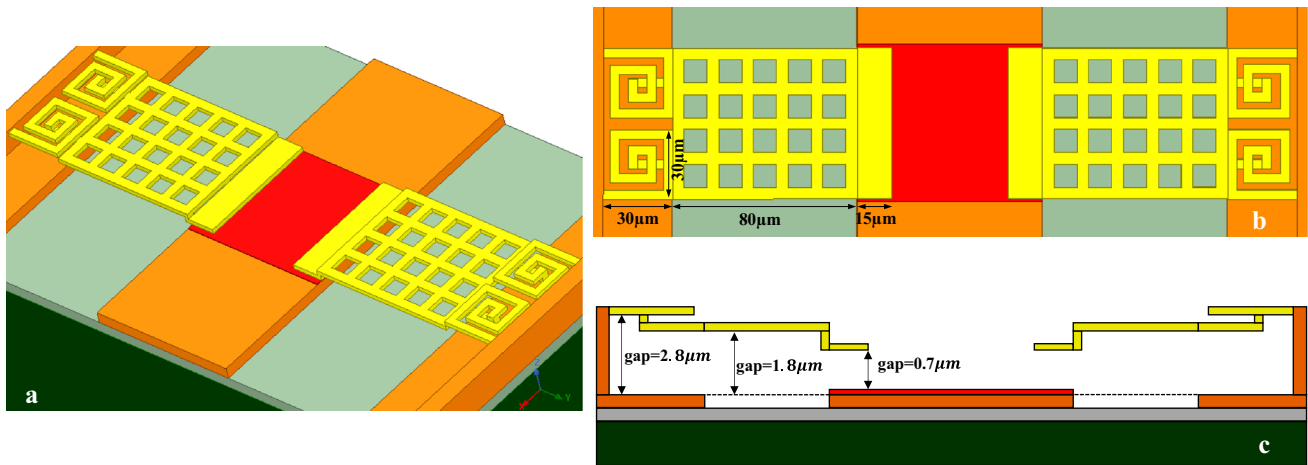


Fig. 3 a Overall view, b Top view, c Side view of the designed switch

the materials used in the proposed device have been shown in Table 1. By using a special design for the spring and two separate beams in the proposed RF device, the actuation voltage has been reduced to 9.2 V. 3d and 2d views of the double-cantilever type switch have been shown in Fig. 3. Using two bridges in the switch with different CPW dimensions results in the application of the proposed switch in the Ka frequency band.

3 Results and discussion

Electromechanical analysis of all results obtained in this paper have been done by using HFSS and COMSOL software. This section explains the method for reduction of spring stiffness constant that has caused the reduction of the actuation voltage. The stress reduction at different points of the beam and spring has been discussed. The lower stress enhances the life-time of the switch at high cycle times.

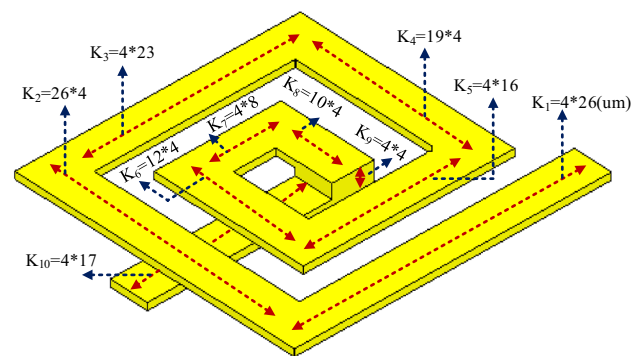


Fig. 4 Dimensions of the designed spiral spring

3.1 Spring design

3.1.1 Reduction of the spring constant

As can be seen in Fig. 4, the spring used in this switch has been designed in the shape of a square spiral spring. The spring constant is calculated using Eqs. (1) and (2) (Rebeiz 2003) for both suspended beams (as shown in Table 2):

Table 2 Calculating of the spring stiffness constant

Thickness	Spring-stiffness (N/m)												
	K_1	K_2	K_3	K_4	K_4	K_5	K_6	K_7	K_8	K_9	K_{10}	K_B	K_{total}
0.8 μm	8.15	14560	11.78	10640	10640	35	6720	280	5600	9611	26.74	3.6	14.4

$$K = \frac{EWt^3}{L^3} \quad (1)$$

$$\frac{1}{K_B} = \frac{1}{K_1} + \frac{1}{K_2} + \frac{1}{K_3} + \dots \quad (2)$$

where K is the spring stiffness constant, E is Young's modulus and t and l are thickness and length of each beam.

3.1.2 Reduction of the stress

Generally, in many RF MEMS switches, the life-time of the switch is reduced after the mechanical force is applied to the beam, due to the tensile that is exerted to interface between the beam and spring. To solve this problem, one solution could be to use a spring structure with two sections in two parallel planes with height differences, which leads to the distribution of the stress in all the spring surface. As can be seen in Fig. 5a, the stress in most points of the spring surface is between 10 MPa and 15 MPa, which is

reduced to less than half compared to the other spring structures reported previously (Rebeiz 2003; Shekhar et al. 2017; Sravani and Rao 2018). Given that sometimes to increase the switching speed, the applied force to the beam has to be greater than the actuation voltage, the proposed a spring design allows us to double the applied force to the beam when needed, while the life-time of the switch does not decrease. As shown in Fig. 5a, the highest stress and the lowest stress have been applied to the spring and the membrane, respectively. Therefore, for reducing the stress in the switch a special notice should be given to the spring design. From Fig. 5a, it can be seen that only the stress of few points of the spring get to 25 MPa [Standard Value (Rebeiz 2003)] and the stresses of the rest of the points are less than that. Also by looking at Fig. 5b, one can see the performance of the designed spring after the electrostatic force is applied to the beam. It has been shown that the proposed design reduces the stress in the switch as mentioned above.

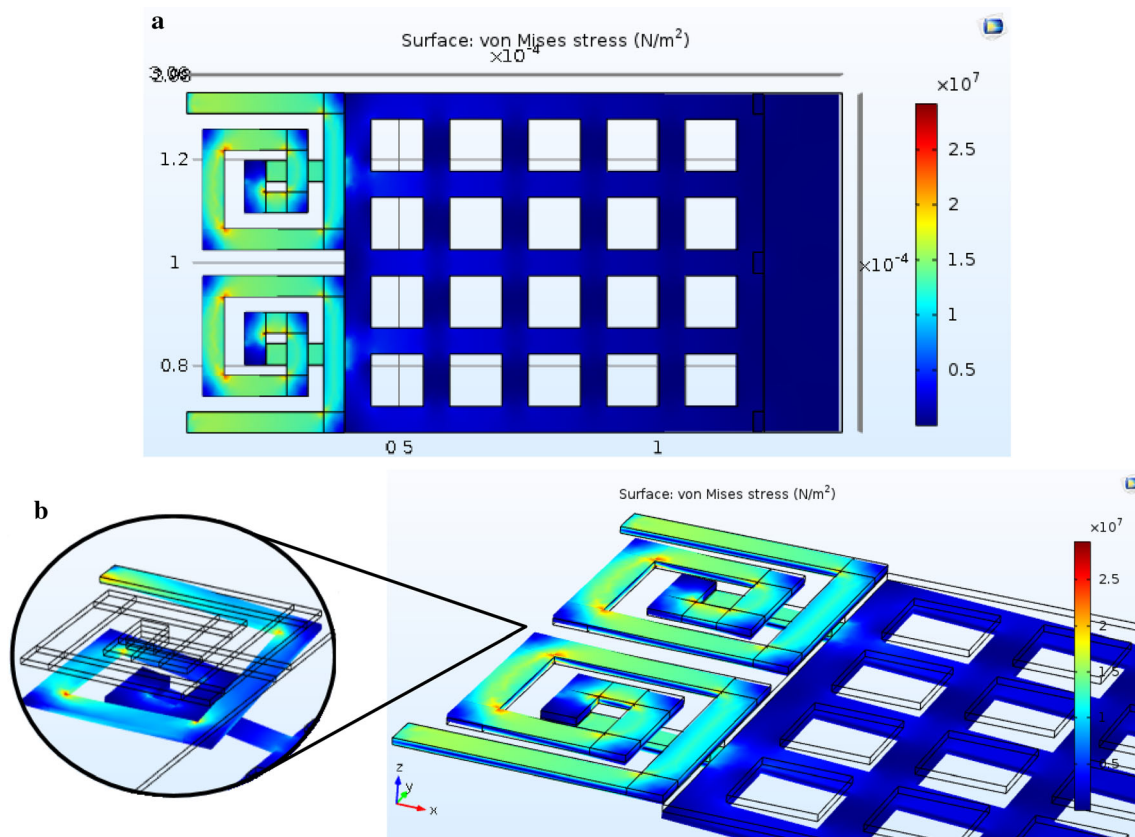


Fig. 5 a Stress profile analysis in the designed spring, b performance of the spring structure from side view

3.2 Actuation voltage

The actuation voltage is the minimum voltage required to place the beam on the T-line which can be achieved by four mechanisms: electrostatic, electromagnetic, electro-thermal, and piezoelectric actuation. Electrostatic actuation, due to its smaller size, lower power consumption and easier fabrication steps is preferred over other mechanisms. The voltage needed to actuate an RF MEMS switch can be calculated using the following equation (Rebeiz 2003), which depends on the air gap, contact area, and spring stiffness constant.

$$V_p = \sqrt{\frac{8k_{total}g_0^3}{27\epsilon_0A}} \tag{3}$$

where k_{total} is the spring coefficient, g_0 is the air gap between the membrane and the dielectric layer, ϵ_0 is the permittivity of vacuum and A illustrates the cross-sectional area of the membrane and the T-line in the down-state. The pull-in voltage is directly related to the air gap (g_0) and the spring stiffness coefficient (k_{total}). The spring constant was explained in the previous section and it was shown that according to Eq. (3) the actuation voltage reduces with the reduction of the spring constant. Figure 6 shows the amount of the actuation voltage versus the air gap variations. As can be seen, after passing 0.7 μm , the bridge comes into contact with the T-line. Figure 7 shows the amount of beam displacement after applying the actuation voltage. Maximum displacement is at the tip of the beams. The displacement decreases along the switch from the tip of the beam to the anchors. Opposite to the displacement, the stress distribution increases from the free tip to the anchors.

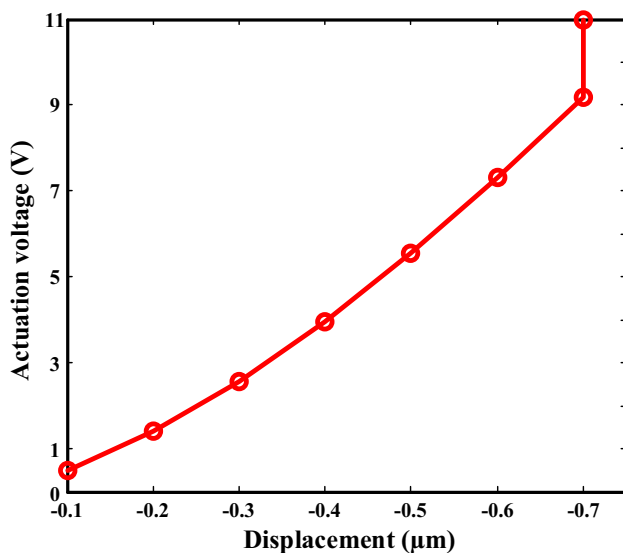


Fig. 6 Actuation voltage for different gaps

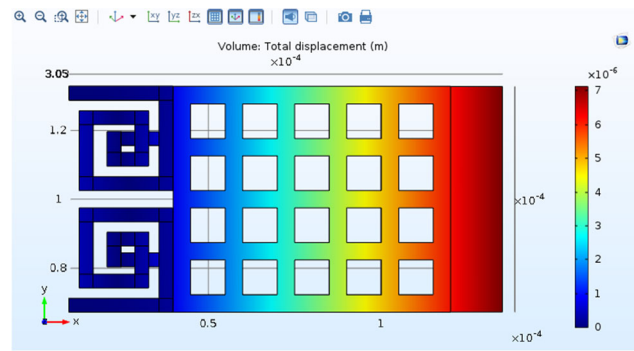


Fig. 7 Amount of displacement after applying the voltage

3.3 Capacitive ratio

To obtain the capacitive ratio, the UP-state and the DOWN-state capacitance must first be calculated according to Eq. (4). After the pull-in voltage is applied, the beam is placed on the dielectric layer and the device switches to the ON-state. In this case, we can obtain the down-state capacitance using Eq. (5). After disconnection of the pull-in voltage and removing the electrical field, the beam returns to its original state (UP-state) and the device is switched to the OFF-state. In this case, using the Eq. (6), the UP-state capacitance can be calculated (Rebeiz 2003):

$$CR = \frac{C_{down}}{C_{up}} \tag{4}$$

$$C_{down} = \frac{\epsilon_0\epsilon_r A}{t_d} \tag{5}$$

$$C_{up} = \frac{\epsilon_0 A}{g_0 + \frac{t_d}{\epsilon_r}} \tag{6}$$

where t_d and ϵ_r are dielectric thickness and dielectric constant, respectively. According to the relationships mentioned above, the dielectric thickness and the air gap have the most impact on the down-state and up-state capacitances, respectively. Figure 8 shows the variation of the down-state capacitance versus the dielectric thickness, whereby the down-state capacitance is 1.55 pF when $t_d = 0.1 \mu\text{m}$. When the bridge is placed on the dielectric layer, a down-state capacitance is created. In this case, since there is no gap between the bridge and the dielectric layer, g_0 is ignored [see Eq. (5)]. As shown in Eq. (5), with reducing dielectric thickness, the down-state capacitance increases and this is because the beam creates more capacitance by getting closer to the transmission line. That's why metal-to-metal switches have more down-state capacitance than capacitive-type switches. Also, in Fig. 9 the variations of the up-state capacitance versus the air gap have been shown. The up-state capacitance is 24.26 fF when the air gap is equal to 0.7 μm . Due to the gap between the beam and the dielectric layer in the up-state, g_0

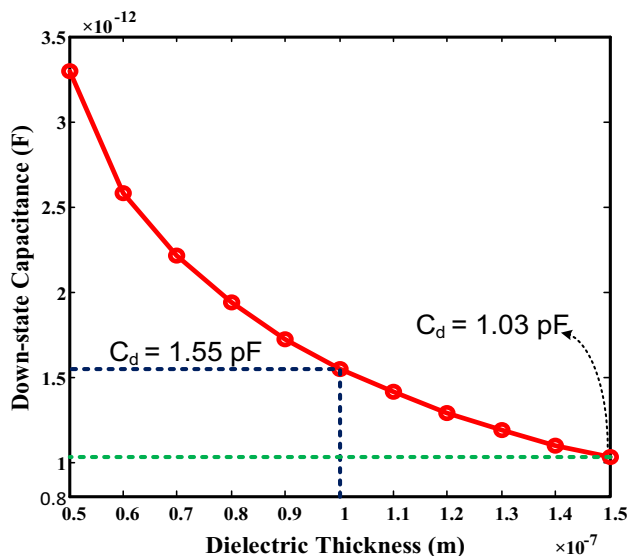


Fig. 8 Dielectric thickness versus down-state capacitance

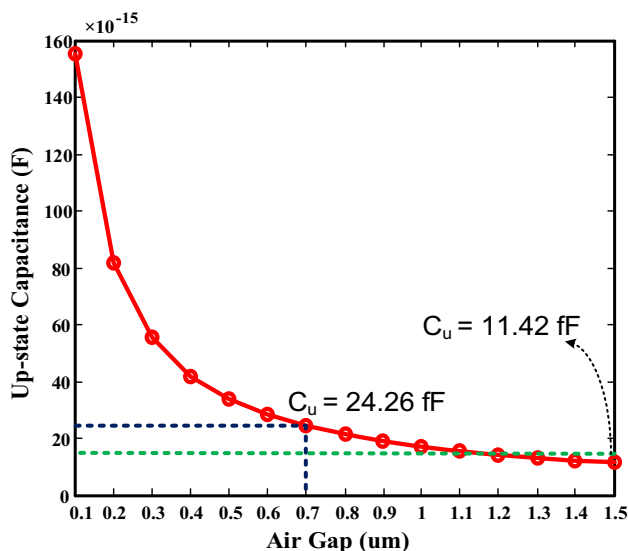


Fig. 9 Air gap versus. up-state capacitance

plays an important role in changing the up-state capacitance [Eq. (6)]. In Fig. 9, different capacitance amounts can be seen while the device switches from up-state to down-state.

3.4 Resonance frequency

One of the most important parameters for determining switching time and quality factor in RF MEMS switches is the resonant frequency of the switch. If the resonant frequency is high, it leads to optimal switching time, and if the resonance frequency is low, it increases the quality factor. In Fig. 10, six resonance modes for the proposed structure and their corresponding resonant frequencies have

been shown. Among the possible motion mechanisms shown for the switch, can be seen that the first mode is more similar to the normal motion mode of MEMS switches. Hence, the resonance frequency of the proposed switch is 10.089 kHz. As is known, the spring stiffness constant and the effective mass of the beam play the most important role in determining the resonance frequency. Equation (7) can also be used to obtain the resonance frequency of the switch (Rebeiz 2003):

$$F = \frac{1}{2\pi} \sqrt{\frac{k}{m}} \tag{7}$$

where F is the resonance frequency, k is the spring stiffness constant and m is the effective mass of the beam.

Calculations show that the resonant frequency obtained for the proposed switch by using Eq. (7) is 10 kHz which is in a very good agreement with the numerical simulation result.

3.5 Switching and release time

The time that takes for the beam to switch from up-state to down-state is called switching time, and the time it takes to switch from down-state to up-state is called release time. According to Eq. (8), the switching time depends on the actuation voltage and the resonance frequency (Rebeiz 2003):

$$t_{pi} = \frac{3.67 \times V_P}{V_S \times 2\pi \times F} \tag{8}$$

where t_{pi} is the switching time, V_P is the actuation voltage, $V_S = 1.6V_P$ and F is the resonance frequency. Release time is obtained from the following equation (Rebeiz 2003):

$$t_{pu} = \frac{1}{4F} = \frac{\pi}{2} \sqrt{\frac{m}{k}} \tag{9}$$

where t_{pu} is the release time (pull-up time). For better understanding of the above concepts, the switching time variations versus the beam thickness are shown in Fig. 11.

3.6 Damping ratio and quality factor

To calculate the quality factor according to Eq. (10), damping ratio, spring stiffness coefficient and resonance frequency are required (Rebeiz 2003):

$$Q = \frac{k}{2\pi F b} \tag{10}$$

where b is the damping ratio. The damping ratio is (Rebeiz 2003):

$$b = \frac{3 \mu A^2}{2 \pi g_0^3} \tag{11}$$

Fig. 10 The first six modes of resonance frequency in the proposed device: **a** resonant mode 1, **b** resonant mode 2, **c** resonant mode 3, **d** resonant mode 4, **e** resonant mode 5, **f** resonant mode 6

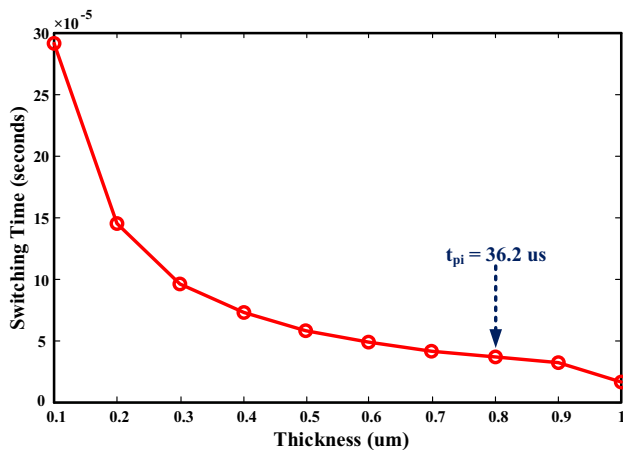
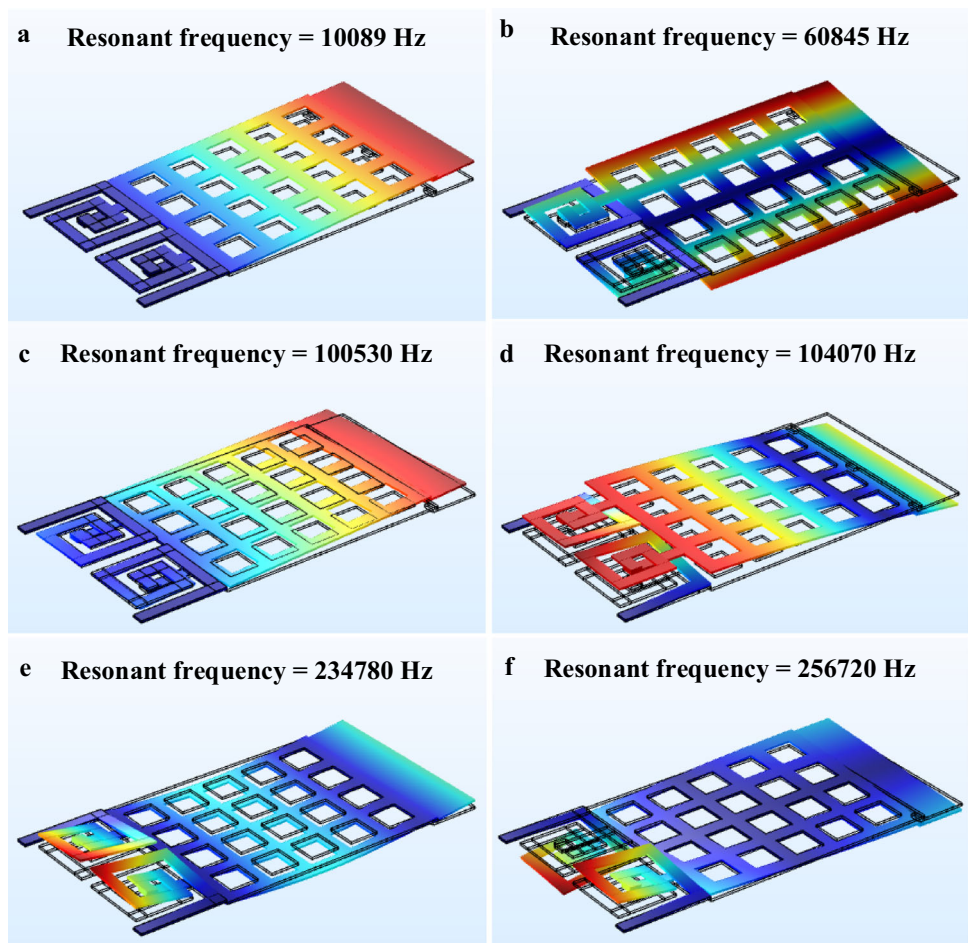


Fig. 11 The switching time for different beam thicknesses in the proposed device

where μ is the viscosity of the air, A is the cross-sectional area and the air gap between the beam the dielectric layer is g_0 . According to Eq. (10), by increasing the spring constant and then increasing the reliability of the switch, a higher quality factor can be achieved.

Figure 12 shows the damping ratio of the proposed switch versus the air gap. As illustrated, the damping ratio reduces with increasing air gap, which is desirable because

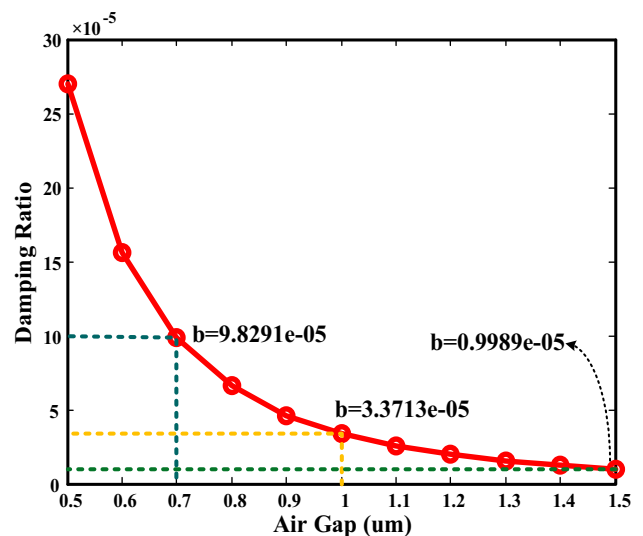


Fig. 12 Amount of damping ratio for different air gap between dielectric layer and the beam

it improves the reliability of the switch and prevents self-actuation (due to events such as shaking). It should be noted, however, that excessive gap increases the actuation voltage and switching time, which is not desirable. In the proposed switch, the damping ratio is equal to $9.8e-05$. This will result in a very good quality factor.

Figure 13 shows the quality factor with respect to the thickness of the aluminum beam. It can be seen that a high quality factor has been obtained for this switch (2.3). This is due to the high thickness of the beam and the low damping coefficient which lead to the long life-time and high reliability of the switch. Recently, in some fabricated switches (Shekhar et al. 2017), the quality factor has been reported between 1 and 1.5 or even less than 1 in some simulations (Sravani et al. 2019a, b).

3.7 RF performance analysis

Many MEMS switches use two methods to increase isolation and reduce losses. The first is that by increasing the cross-sectional area of the beam and the transmission line, increase the signal transmitted to the ground is increased which increases the isolation. The second is the choice of a high conductivity material as the beam. This will allow the signal to be transmitted more easily and in turn improves the isolation. The disadvantages of these two methods are the increased switch size and the heavier beam. In this paper, we have designed a beam with smaller cross-sectional area compared to the previous works. We have selected Aluminum as the beam material which is lighter than gold. The study shows that the less conductivity of the aluminum does not degrade the switch performance and it still exhibit acceptable S-parameters. Excellent

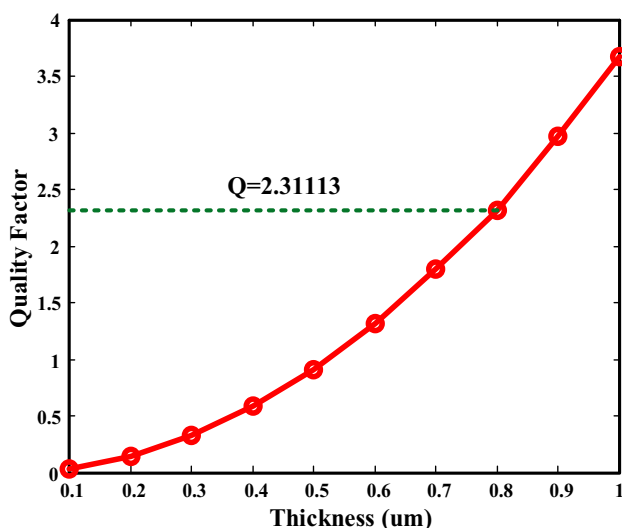


Fig. 13 Amount of quality factor for different thicknesses of the aluminum beam

S-parameters have been obtained for the proposed switch which can be seen in Table 3. The reason for obtaining such good s-parameters is the special design of the spring and the beam. As shown in Fig. 14a, the isolation and the insertion loss are -57 dB and -0.37 dB, respectively. Also the proposed switch has the return loss equal to -18 dB (see Fig. 14b in 33.5 GHz).

3.8 The effect of passive elements on the switch isolation

In recent years, many MEMS switches have been simulated and fabricated, but none have investigated the results of the switch after being placed in an electrical circuit. This has caused the practical measurements to be different from simulation results. In reality, RF MEMS switches must be placed in an electrical circuit in the presence of passive and active elements. It can be claimed that in all previous works on RF MEMS switches, both in simulation and fabrication, the performance of the switch has been analyzed without considering the impact of other components on the circuit.

As is evident, the switch in an electrical circuit is adjacent to many passive and active elements, including inductors, resistors, capacitors and transistors. In this paper, we investigate the effect of inductor and capacitor on the switch isolation in order to bring the results of the switch simulation closer to reality. Figures 15 and 16 illustrate the isolation variations after the capacitor and the inductor are inserted on the input of the T-line, respectively.

4 Conclusion

A novel RF MEMS switch was designed. While the switch has a light weight and small size, it has excellent results due to its special spring design. The switch design is based on a two separate beam sections anchored by means of two springs. The design of the springs extended the stiffness constant to 14.4, resulting in a high quality factor of about 2.3. Also, the stress in the switch was reduced because of the proposed spring design. The actuation voltage and capacitive ratio obtained 9.2 V and 64, respectively. Isolation, insertion loss and return loss were obtained -57 dB, -0.3 dB and -18 dB, respectively. The switching time was calculated to be 36.2 μ s for the beam thickness of 0.8 μ m. As an innovation in this paper, the effect of capacitors and inductors on the input of the transmission line on the switch isolation has been investigated which helps to bring the switch results closer to the reality.

Table 3 Comparison of the proposed device parameters with previous works

Electrostatic RFMEMS switch	Mahameed and Rebeiz (2011)	Mafinejad et al. (2017)	Ziaei et al. (2015)	This work
Actuation voltage	23.6 V	20 V	60 V	9.2 V
Return loss	− 9.23 dB@40 GHz	− 20 dB@24 GHz	−	− 18 dB@33 GHz
Isolation	− 35.75 dB@40 GHz	− 18 dB@24 GHz	− 30 dB@10 GHz	− 57 dB@33 GHz
Insertion loss	− 0.68 dB@40 GHz	− 0.9 dB@24 GHz	−	− 0.3 dB@33 GHz
C_{ratio}	9.87	12–20	77.5	64

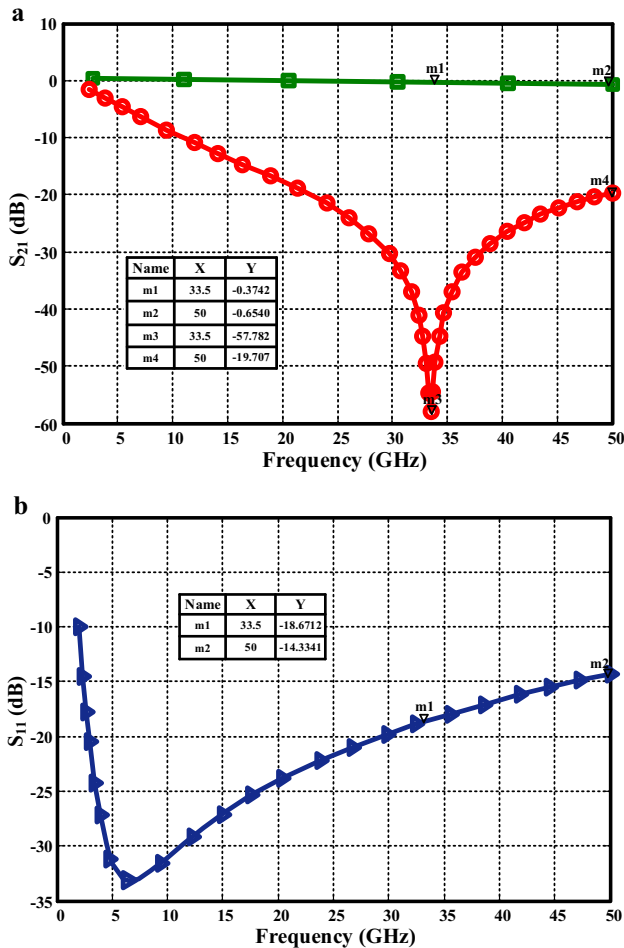


Fig. 14 **a** Insertion loss (green) and isolation (red) **b** Return loss of the proposed device (color figure online)

References

Amiri P, Kordrostami Z (2018) Sensitivity enhancement of MEMS diaphragm hydrophones using an integrated ring MOSFET Transducer. *IEEE Trans Ultrason Ferroelectr Freq Control* 65(11):2121–2130

Ansari HR, Behnam Taghaddosi M (2019) Optimization and development of the RF MEMS structures for low voltage, high isolation and low stress. *Analog Integr Circuits Signal Process* 101:659–668

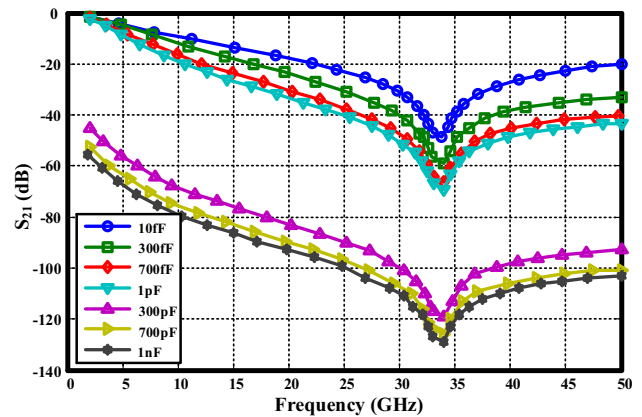


Fig. 15 The isolation variations after the capacitor is inserted on the input of the T-line

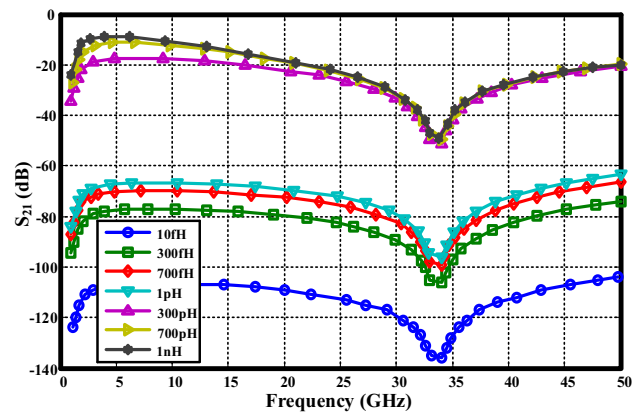


Fig. 16 The isolation variations after the inductor is inserted on the input of the T-line

Ansari HR, Khosroabadi S (2018) Low actuation voltage RF MEMS shunt capacitive switch with high capacitive ratio. In: 26th Iranian conference on electrical engineering

Ansari HR, Khosroabadi S (2019) Design and simulation of a novel RF MEMS shunt capacitive switch with a unique spring for Ka-band application. *Microsyst Technol* 25(2):531–540

Anuroop Bansal D, Kumar P, Kumar A, Khushbu Rangra K (2018) Low temperature epoxy bonding for RF MEMS capacitive switch. *Microsyst Technol* 25(8):3047–3051

Ghoddus H, Kordrostami Z (2018) Harvesting the ultimate electrical power from mems piezoelectric vibration energy harvesters: an optimization approach. *IEEE Sens J* 18(21):8667–8675

- Ghoddus H, Kordrostami A, Amiri P (2019) Performance enhancement of MEMS-guided four beam piezoelectric transducers for energy harvesting and acceleration sensing. *Int J Mod Phys B* 33(18):1950192
- Khodadady K, Azizolla B (2015) Design and modeling of a novel RF MEMS series switch with low actuation voltage. *Microsyst Technol* 22(12):2921–2929
- Kordrostami Z, Roohizadegan S (2018) A groove engineered ultralow frequency piezomems energy harvester with ultrahigh output voltage. *Int J Mod Phys B* 32(20):1850208
- Kordrostami Z, Roohizadegan S (2019) Particle swarm approach to the optimisation of trenched cantilever-based MEMS piezoelectric energy harvesters. *IET Sci Meas Technol* 13(4):582–588
- Lakshmi S, Manohar P, Naga SP (2016) Optimization of structures of DC RF MEMS series switches for low actuation. *Microsyst Technol* 23(7):2371–2379
- Mafinejad Y, Kouzani AZ, Nassabi M, Lim Y, Mafinezhad K (2015) Characterization and optimization to improve uneven surface on MEMS bridge fabrication. *Displays* 37:54–61
- Mafinejad Y, Kouzani A, Mafinezhad K, Hosseinezhad R (2017) Low insertion loss and high isolation capacitive RF MEMS switch with low pull-in voltage. *Int J Adv Manuf Tech* 93:661–670
- Mafinejad Y, Ansari HR, Khosroabadi S (2019) Development and optimization of RF MEMS switch. *Microsyst Technol* 26:1253–1263
- Mahameed R, Rebeiz GM (2011) RF MEMS capacitive switches for wide temperature range applications using a standard thin-film process. *IEEE Trans Microw Theory Tech* 59(7):1746–1752
- Molaei S, Ganji BA (2017) Design and simulation of a novel RF MEMS shunt capacitive switch with low actuation voltage and high isolation. *Microsyst Technol* 23:1907–1912
- Rao KS, Chand CG, Sravani KG, Prathyusha D, Naveena P, Lakshmi GS, Kumar PA, Narayana TL (2019) Design, modeling and analysis of perforated RF MEMS capacitive shunt switch. *IEEE Access* 7:74869–74878
- Rebeiz GM (2003) *RF MEMS: theory, design and technology*. Wiley, Hoboken
- Rebeiz GM, Entesari K, Reines IC, Park SJ, El-Tanani M, Grichener A, Brown AR et al (2009) Tuning in to RF MEMS. *IEEE Microwave Theory Tech Soc* 10:55–72
- Shekhar S, Vinoy KJ, Ananthasuresh GK (2017) Surface-micromachined capacitive RF switches with low actuation voltage and steady contact. *J Microelectromech Syst* 26:643–652
- Sravani KG, Rao KS (2018) Analysis of RF MEMS shunt capacitive switch with uniform and non-uniform meanders. *Microsyst Technol* 24(2):1309–1315
- Sravani KG, Prathyusha D, Rao KS, Kumar PA, Lakshmi GS, Chand CG, Naveena P, Thalluri LN, Guha AK (2019a) Design and performance analysis of low pull-in voltage of dimole type capacitance RF MEMS shunt switch for Ka-band. *IEEE Access* 7:44471–44488
- Sravani KG, Rao KS, Prathyusha D, Sai Kiran BV, Kumar BS, Kumar RP, Tarun KS (2019b) Design and performance analysis of double cantilever type capacitive shunt RF MEMS switch. *Microsyst Technol* 26:345–352
- Uvarov IV, Kupriyanov AN (2018) Stiction-protected MEMS switch with low actuation voltage. *Microsyst Technol* 25(8):3243–3251
- Ziaei A, Bansropun S, Martins P, Baillif ML (2015) Fast high power capacitive RF-MEMS switch for X-Band applications. In: *Proceedings of 45th European solid-state device research conference*, pp 153–155

Publisher's Note Springer Nature remains neutral with regard to jurisdictional claims in published maps and institutional affiliations.